



Molecular Crystals and Liquid Crystals

Publication details, including instructions for authors and subscription information:

<http://www.tandfonline.com/loi/gmcl20>

A Facile Synthesis of PMMA-SiO₂ Nanocomposites via Surface Initiated Radical Polymerization

Long Giang Bach^a, Md. Rafiqul Islam^a, Yeon Tae Jeong^a, Ha Soo Hwang^b & Kwon Taek Lim^a

^a Department of Imaging System Engineering, Pukyong National University, Busan, 608-737, Republic of Korea

^b Packaging Technology Serve Center, Korea Institute of Industrial Technology (KITECH), Bucheon, 421-742, Republic of Korea
Version of record first published: 30 Aug 2012.

To cite this article: Long Giang Bach, Md. Rafiqul Islam, Yeon Tae Jeong, Ha Soo Hwang & Kwon Taek Lim (2012): A Facile Synthesis of PMMA-SiO₂ Nanocomposites via Surface Initiated Radical Polymerization, *Molecular Crystals and Liquid Crystals*, 565:1, 78-87

To link to this article: <http://dx.doi.org/10.1080/15421406.2012.692262>

PLEASE SCROLL DOWN FOR ARTICLE

Full terms and conditions of use: <http://www.tandfonline.com/page/terms-and-conditions>

This article may be used for research, teaching, and private study purposes. Any substantial or systematic reproduction, redistribution, reselling, loan, sub-licensing, systematic supply, or distribution in any form to anyone is expressly forbidden.

The publisher does not give any warranty express or implied or make any representation that the contents will be complete or accurate or up to date. The accuracy of any instructions, formulae, and drug doses should be independently verified with primary sources. The publisher shall not be liable for any loss, actions, claims, proceedings, demand, or costs or damages whatsoever or howsoever caused arising directly or indirectly in connection with or arising out of the use of this material.

A Facile Synthesis of PMMA-SiO₂ Nanocomposites via Surface Initiated Radical Polymerization

LONG GIANG BACH,¹ MD. RAFIQUUL ISLAM,¹ YEON TAE
JEONG,¹ HA SOO HWANG,² AND KWON TAEK LIM^{1,*}

¹Department of Imaging System Engineering, Pukyong National University,
Busan 608-737, Republic of Korea

²Packaging Technology Serve Center, Korea Institute of Industrial Technology
(KITECH), Bucheon 421-742, Republic of Korea

Well-defined core-shell structured poly(methyl methacrylate) grafted silica nanocomposites (PMMA-g-SiO₂) were synthesized via thiol-lactam initiated radical polymerization by employing a grafting from protocol. Spherical SiO₂ nanoparticles were reacted with 3-mercaptopropyl-trimethoxysilane in order to prepare thiol functionalized SiO₂ nanoparticles (SiO₂-SH). Subsequently, the surface initiated polymerization was accomplished by using two component initiating system comprising SiO₂-SH and butyrolactam. The anchoring of PMMA onto the surface of SiO₂ nanoparticles was ascertained by FTIR and XPS analyses. A uniform and spherical core-shell structure of PMMA-g-SiO₂ was revealed from TEM and SEM images. The GPC analysis demonstrated that the molecular weight of PMMA was a function of both monomer conversion and polymerization time. DLS also confirmed that the hydrodynamic diameter of the nanocomposites was directly related to the polymerization time. An improved thermal property of the polymer matrix with incorporating SiO₂ nanoparticles was revealed by TGA study.

Keywords Silica nanoparticles; poly(methyl methacrylate); hybrid nanocomposites; polymer brush; core-shell; surface initiated polymerization

Introduction

Over recent years, an increasing interest has been focused on the preparation and application of polymer/inorganic nanocomposites, which can combine the properties of inorganic particles such as mechanical strength and thermal stability with the processability and flexibility of organic polymers. The composites possess high potential for applications in many fields, including chemistry, physics, electronic, optics, material science, and biomedical science [1–4]. Among various nanocomposites, the preparation of core-shell composite materials having a functional polymer with inorganic materials have received particular attention due to their great promising applications [5–8]. Poly (methyl methacrylate) (PMMA) is a functional polymer which has been used in a diverse fields such as biomaterials, optoelectronics and optical fibers because of its good optical and mechanical properties [9].

*Address correspondence to Prof. Kwon Taek Lim, Department of Imaging System Engineering, Pukyong National University, Busan 608-737, Korea (ROK). Tel.: (+82)51-629-6409; Fax: (+82)51-629-6408. E-mail: ktlim@pknu.ac.kr

To date, many techniques for grafting polymer on SiO₂ surfaces have been developed based on several surface initiated radical polymerization such as atom transfer radical polymerization, nitroxide-mediated polymerization, and reversible addition-fragmentation transfer polymerization, and so on [10–13]. Recently, we reported that thiol groups could initiate polymerization with the aid of butyrolactam (BL) [14,15]. Considering the above findings into accounts, it would be a efficient strategy to develop a one-step direct anchoring of initiator moiety, preferably thiol groups to SiO₂ surface that eventually enable the preparation of SiO₂ nanocomposites with high density PMMA.

In this paper, we demonstrate a convenient synthesis of structurally well-defined PMMA grafted SiO₂ nanoparticles (PMMA-*g*-SiO₂) with a core-shell nanostructure using a two component initiation system comprising of thiol-functionalized silica (SiO₂-SH) and BL.

Experimental

Materials

NH₄OH (25 wt.% aqueous solution), (3-mercaptopropyl) trimethoxysilane (MPTMS), butyrolactam (BL), tetraoctylammonium bromide (TOAB), ethanol, methanol, toluene, tetrahydrofuran (THF), tetraethylorthosilicate (TEOS, 95%) were purchased from Aldrich and used as received. Methyl methacrylate (MMA) was purified by passing the liquid through a neutral alumina column to remove the inhibitor prior to use.

Synthesis of SiO₂ Nanoparticles

The SiO₂ nanoparticles were synthesized by using the Stober procedure [16]. 200 mL of absolute ethanol and 15 mL of 28 wt.% ammonia solution were placed into a round flask. The mixture was stirred at 300 rpm to homogenize the mixture, which was then heated to 60°C. Subsequently, 6 mL of TEOS was added to the solution and the reaction was carried out for 24 h. The product was isolated by an ultracentrifuge operated at 10000 rpm for 30 min and dried in vacuum at 40°C for 24 h.

Preparation of the Surface-Modified SiO₂ Nanoparticles

The surface of SiO₂ was coated with MPTMS by a silanization reaction to obtain thiol functionalized silica nanoparticles according to reported procedure [17]. In a typical procedure, an excess of MPTMS was added to 10 g of the SiO₂ particles dispersed in 100 mL of toluene, and the mixture was stirred for 24 h in an argon atmosphere. Modified SiO₂-SH was isolated by an ultracentrifuge and washed several times with toluene to remove the unreacted MPTMS. Modified SiO₂-SH was dried in vacuum at 40°C for overnight.

Surface Thiol-Lactam Initiated Radical Polymerization (TLIRP) of MMA from the Surface of SiO₂ nanoparticles

A typical procedure for synthesizing PMMA-*g*-SiO₂ nanocomposites by TLIRP is as follows: 1 g of MMA, 0.2 g of SiO₂-SH, 0.5 g of BL, 2 mL of THF and a Teflon-coated stir bar were placed in a 25 mL round flask equipped with a reflux condenser. The flask was purged with nitrogen, heated to 80°C and kept stirring. At the end of the reaction,

the viscosity increased dramatically. After the desired time, the flask was cooled to room temperature and the reaction mixture was precipitated in hexane. The product was filtered and dried in a vacuum oven. Then yield was determined gravimetrically. The polymer product was diluted in toluene and centrifuged to collect the PMMA-*g*-SiO₂. This cycle of centrifugation and redispersion in toluene was repeated twice to obtain the polymer grafted SiO₂ free from the unbound polymer.

To evaluate the dependence of number-averaged molecular weight (M_n) and polydispersity index ($PDI = M_w/M_n$) values of the grafted PMMA on polymerization time, the PMMA chains were cleaved from the SiO₂ surface as follows: 50 mg of the PMMA-*g*-SiO₂ particles and 50 mg of TOAB were dissolved in 5 mL of toluene in a polyethylene flask. A 5% HF aqueous solution was then added to the mixture. The mixture was stirred vigorously for 24 h. The cleaved PMMA in the organic layer was precipitated in hexane.

Measurements

Transmission Electron Microscopy (TEM) images were recorded using a Hitachi H-7500 instrument operated at 80 kV. A drop of the sample dispersed in distilled toluene was placed on a copper grid and drying. The changes in the surface chemical bonding of functionalized SiO₂ nanoparticles, SiO₂-SH, and PMMA-*g*-SiO₂ hybrid particles were captured by Fourier Transformed Infrared Spectrophotometry (FT-IR) using a BOMEM Hartman & Braun FT-IR Spectrometer in the frequency range of 4000–400 cm⁻¹. The morphology and elemental analysis of the hybrids were carried out by using Field Emission Scanning Electron Microscopy (FE-SEM) images equipped with an Energy Dispersive X-Ray (EDX) spectrometer (Hitachi JEOL- JSM-6700F system, Japan). Thermogravimetric analysis (TGA) was conducted with Perkin-Elmer Pyris 1 analyzer (USA). Before the test, all the samples were carefully grinded into fine powder. The samples were scanned within the temperature range of 50–800°C at a heating rate of 10°C min⁻¹ under continuous nitrogen flow. Surface composition was investigated using X-ray Photoelectron Spectroscopy (XPS) (Thermo VG Multilab 2000) in ultra high vacuum with Al K α radiation. The crystallographic state of SiO₂ nanoparticles was determined by a Philips X'pert-MPD system diffractometer (Netherlands) with Cu K α radiation. Brunauer–Emmett–Teller (BET) isotherms were obtained with an Autosorb-1 from Quantachrome (United States). The samples were dried at 200°C for 3 h in a vacuum oven and nitrogen was used as the adsorbent. Dynamic laser light scattering (DLS) measurements of the SiO₂ nanocomposites were carried out using a Brookhaven laser light scattering instrument (Brookhaven instruments Corporation), with diode laser (24 mV) at a wavelength of 659 nm at 25°C. The sample solution (1 g/L) was prepared by dispersing the SiO₂ nanoparticles in IPA and allowed to settle down a small portion of agglomerated nanoparticles for 6 h. The scattered light of a vertically polarized laser was measured at an angle of 90 ° and was collected on a Brookhaven BI 9000 AT autocorrelator. GPC was performed using an Agilent 1200 Series equipped with PLgel 5 μ m MIXED-C columns, with THF as the solvent at 30°C. The solution flow rate was 1 mL/min. Calibration was carried out using PMMA standards.

Results and Discussion

Surface Modification of SiO₂ Nanoparticles by MPTMS

To synthesize polymer grafted SiO₂ nanoparticles by TLIRP method, SiO₂ nanoparticles with mean size of 108 nm was first prepared by Stober procedure. The specific surface

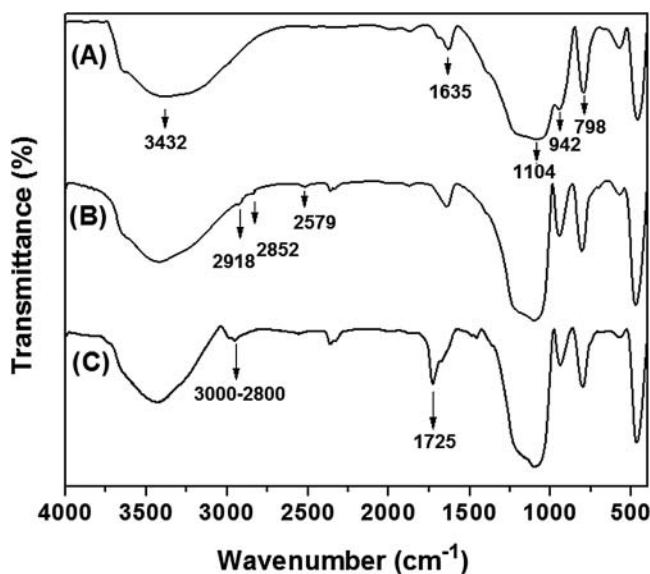


Figure 1. FT-IR spectra of (A) SiO₂ nanoparticles, (B) SiO₂-SH and (C) PMMA-*g*-SiO₂.

area of the SiO₂ nanoparticles was found to be 114 m²/g measured by BET method. SiO₂ nanoparticles were treated with MPTMS and the subsequently removed any free MPTMS by washing with toluene in several times. The FT-IR spectra of the SiO₂ nanoparticles and SiO₂-SH provided clear evidence for the surface modification of SiO₂ nanoparticles by MPTMS as shown in Fig. 1. The strong absorbance at 1104 cm⁻¹ is reasonably attributed to the Si-O-Si stretch of silica. The band at 942 cm⁻¹ is assigned to the Si-OH stretching of silanol groups on the silica particles, while the absorbance at 1635 and 3432 cm⁻¹ are assigned to the surface hydroxyl on the surface of SiO₂ nanoparticles. The MPTMS functionalized silica nanoparticles gave a weak but visible absorption band at 2579 cm⁻¹ assigning for the S-H stretch band, which is not be observed in the absorption spectrum of bare SiO₂ nanoparticles, indicating chemically immobilization of MPTMS on SiO₂ nanoparticles was successfully occurred [17]. The absorption bands for the propyl group are appeared at 2918 and 2852 cm⁻¹ due to the C-H stretching vibrations, further justifying the MPTMS anchored onto SiO₂ nanoparticles. All of the above experimental findings strongly suggest that MPTMS indeed reacted with the OH groups of the SiO₂ surface.

In addition to FT-IR, XPS analysis was carried out to evaluate the surface chemical composition of SiO₂ nanoparticles and SiO₂-SH (Fig. 2). The wide-scan spectrum of the bare SiO₂ surface is dominated by signals attributable to Si, O, and C as shown in Fig. 2A. MPTMS was immobilized on the surface of SiO₂ nanoparticles can offer a condensation reaction to produce a stable initiator monolayer. Figure 2B shows the survey scan spectrum of SiO₂-SH. The major peak component at the binding energy (BE) of 533.6 eV is attributable to O1s, and the minor peak component at the BE of 285.0 eV is assigned to C1s. Meanwhile, peaks at the BE of 154.8 and 103.7 eV correspond to Si2s and Si2p, respectively. The peak of Si2p can be curve-fitted with two peak components with binding energy of 103.7 and 101.9 eV, and these two peaks are attributable to O-Si-O and O-Si-C species, respectively, as shown in Fig. 2C. In the wide-scan spectrum of SiO₂-SH surface (Fig. 2D), the appearance of S2p core-level signals is prominent. The binding energy

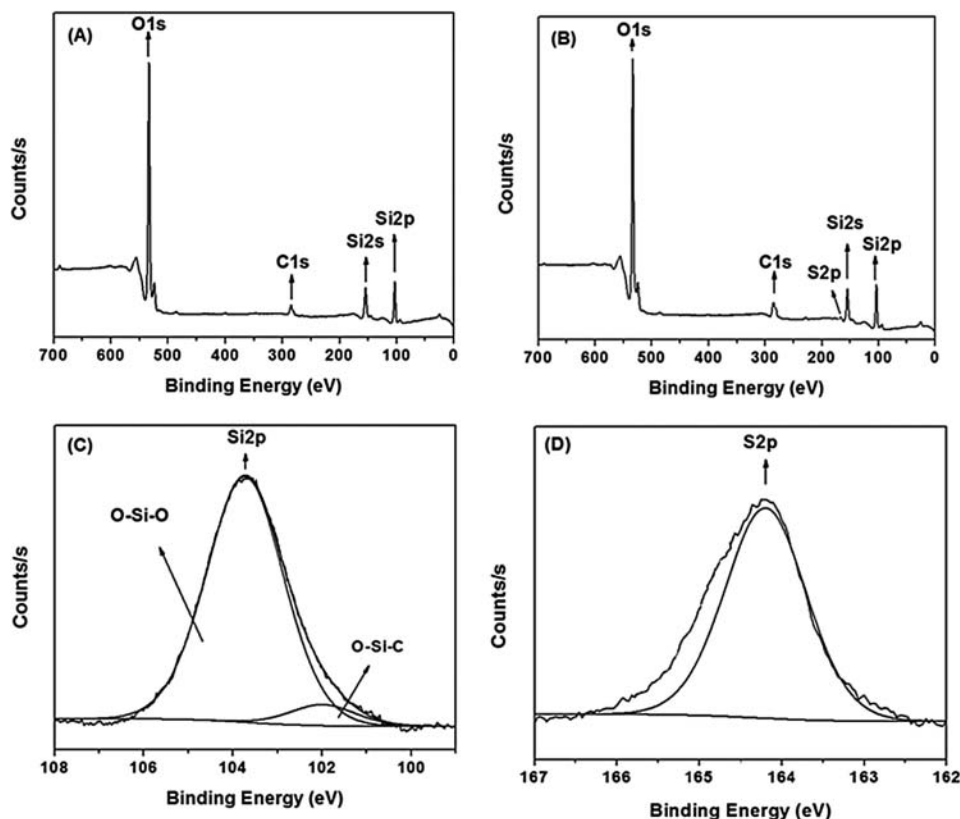


Figure 2. XPS spectra of (A) wide-scan of bare SiO₂, (B) SiO₂-SH, (C) the Si2p core-level spectrum and (D) the S2p core-level spectrum of SiO₂-SH.

of S2p at 164.1 eV demonstrates the existence of S–H groups in SiO₂-SH. The persistence of the S2p species in wide-scan spectrum suggests that a dormant thiol species can be used to initiate the subsequent polymerization *via* TLIRP. Considering the above findings into accounts, it can easily be suggested that the MPTMS has been covalently bonded onto the SiO₂ nanoparticle surfaces.

TGA was employed to determine the amount of MPTMS attached onto SiO₂ nanoparticles (Fig. 5). From the TGA curves, the initial degradation temperature and final degradation temperature were determined. The sample of SiO₂ nanoparticles has a weight loss of around 5.1% of their total weight in the whole temperature range because of the loss of water molecules adsorbed onto the surface and the release of the structural water resulted from the bonded hydroxyl groups. The amount of the grafted MPTMS was determined to be approximately 10.7%, as estimated from the TGA curve in Figure 5B.

Synthesis of PMMA Immobilized SiO₂ Nanoparticles (PMMA-g-SiO₂)

MPTMS-anchored SiO₂ nanoparticles were utilized as initiators for TLIRP, where BL was used as a radical generating agent for polymerization. The core-shell structured PMMA-g-SiO₂ nanocomposites were successfully synthesized by TLIRP protocol and subsequently subjected for characterization by FT-IR, XPS, TGA, GPC, SEM and TEM.

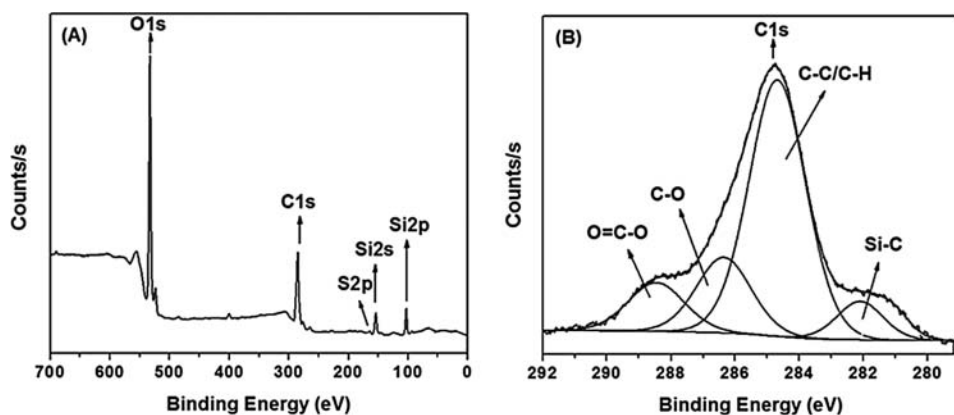


Figure 3. XPS spectra of (A) wide-scan the PMMA-*g*-SiO₂, (B) C1s core-level spectra of PMMA-*g*-SiO₂ surface

The FT-IR spectrum of PMMA-*g*-SiO₂ is shown in Fig. 1C. The PMMA modified SiO₂-SH was confirmed by a new peak appeared at around 1725 cm⁻¹ indicates the characteristic C = O double bond stretching of PMMA. The characteristic bands in the range of 3000 to 2800 cm⁻¹ might ascribe for C-H stretching vibrations of the CH₃ and CH₂ groups of PMMA on the surface of SiO₂ nanoparticles. These results imply that the PMMA was successfully grafted on the surface of SiO₂ nanoparticles.

XPS scans of the PMMA brushes anchored SiO₂ nanoparticles are shown in Fig. 3. The wide-scan of PMMA-*g*-SiO₂ is depicted in Fig. 3A. The Fig. 3B clearly shows the C1s core-level spectra of PMMA-*g*-SiO₂ with four peak components having BE at 282.1, 284.7, 286.3 and 288.5 eV attributable to the Si-C, C-C/C-H, C=O, and O=C-O in alkyl and carboxylate carbon species, respectively. The appearance of C=O and O=C-O components further confirm that PMMA has been successfully grafted onto the SiO₂-SH surface. All these results are consistent with what would be expected of a monolayer of PMMA.

Polymerization on SiO₂-SH particles was attempted for a different reaction time ranging from 5 to 15 h. Due to the low dispersibility of SiO₂-SH in the reaction medium, the solution was slightly cloudy at the initial stages of the TLIRP. The solution was progressively clearer upon polymerization proceeded, because of the formation of PMMA chains on the silica surface. The monomer conversion was reached at more than 62% after polymerization for 15 h. In order to determine the molecular weight of the grafted PMMA and whether the TLIRP polymerization was controlled, the PMMA-*g*-SiO₂ nanocomposites were dispersed in toluene and the SiO₂ cores were etched with 5% aqueous HF. The PMMA chains were isolated from the solution and subjected for analysis by SEC. Figure 4 displays the plots of the number-average molecular weight (*M_n*) and molecular weight distributions (*M_w*/*M_n*) of the grafted PMMA against the overall monomer conversions. By GPC analysis, it can be found that molecular weight of the PMMA increased with increasing monomer conversion, and the molecular weight of the grafted polymer (corresponding to the thickness of the polymeric shell) can be controlled with the polymerization time. GPC analysis of the cleaved PMMA chains (polymerization for 15 h) reveals a number-average molecular weight (*M_n*) of 49 900 and the polydispersity indices is slightly broader (*M_w*/*M_n*, of 1.89).

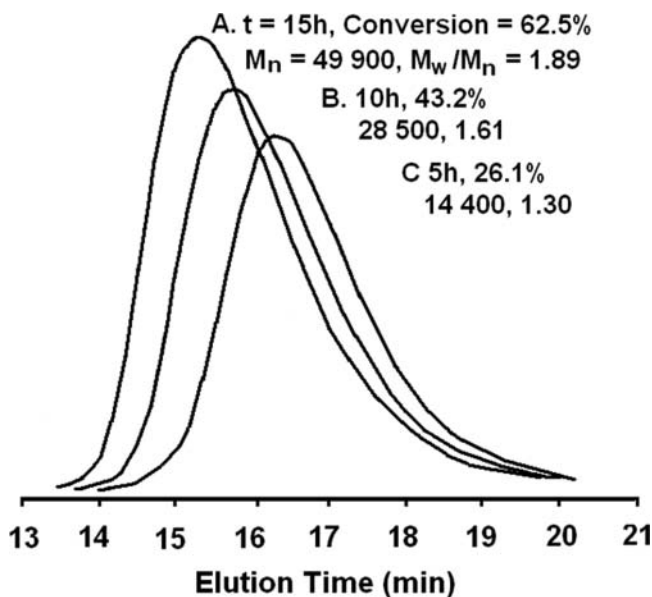


Figure 4. Evolution of GPC traces with polymerization time. PMMA brushes were cleaved from PMMA- g -SiO₂ nanoparticles using HF.

To examine the composition effect on the thermal degradation of the PMMA- g -SiO₂ nanocomposites, TGA analyses were performed for all the samples at the temperature range of 50 to 800°C. TGA curves of SiO₂, SiO₂-SH, PMMA- g -SiO₂ and extracted PMMA from the silica nanoparticles are shown in Fig. 5. As shown in Fig. 5C–E, the amount of polymer

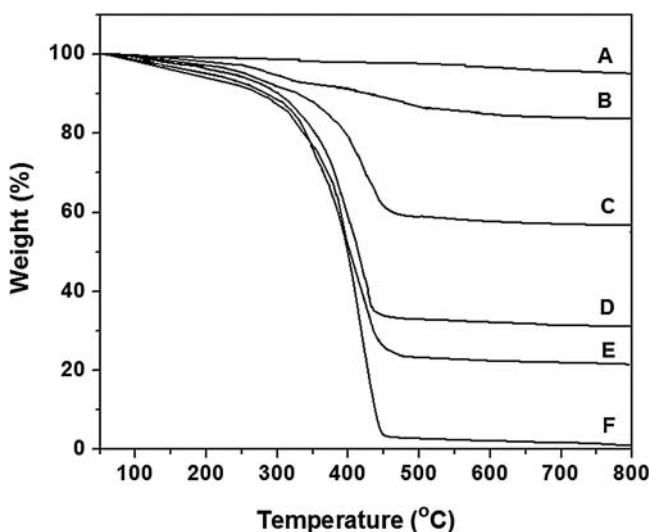


Figure 5. TGA analysis of (A) SiO₂, (B) SiO₂-SH, (C, D, and E) PMMA- g -SiO₂ after polymerization time of 5 h, 10 h, and 15 h, respectively and (F) grafted PMMA cleaved from PMMA- g -SiO₂ after polymerization for 15 h.

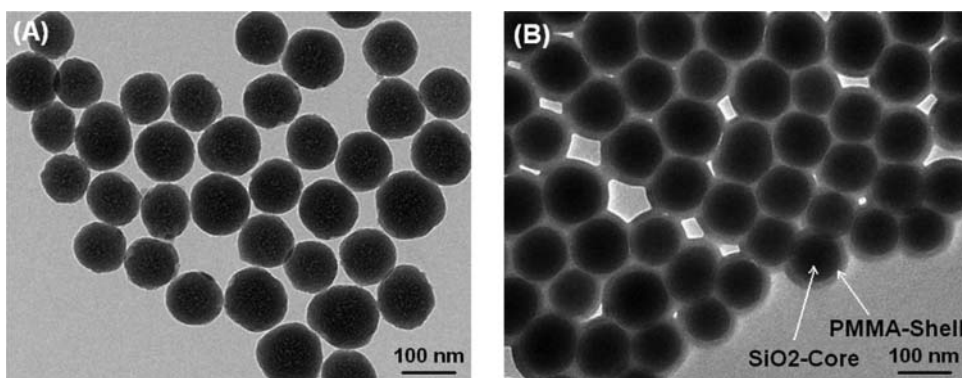


Figure 6. TEM images of (A) bare SiO₂ nanoparticles, and (B) PMMA-g-SiO₂.

on silica surface increases with polymerization time. TGA curve of PMMA-g-SiO₂ shows a major decomposition at the temperature from 250 to 430°C corresponding to surface grafting from the silica surface. The weight loss of PMMA-g-SiO₂ is estimated to be 43.6% after polymerization for 5 h (Fig. 5C) and increased to 67.9% after polymerization for 10 h (Fig. 5D). After polymerization for 15 h, the relative amount of PMMA grafted silica was reached to 78.9% (Fig. 5E). The pure PMMA (extracted from SiO₂ nanocomposites) decomposed completely at about 420°C as shown in Fig. 5F. The content of the polymer calculated from the TGA curve demonstrates a moderate degree of functionalization of PMMA on the surface of the SiO₂ nanoparticles by the *grafting from* approach. It could be concluded that the addition of the nanoparticles significantly improved the thermal properties of the polymer.

The structure and morphology of core-shell PMMA-g-SiO₂ nanocomposites were characterized using TEM and SEM analyses. Figure 6 represents the TEM photographs of the SiO₂ nanoparticles and PMMA-g-SiO₂ nanocomposites. SiO₂ nanoparticles of average particle size 108 nm which are almost spherical in shape with slightly broad particle size distribution as measured by TEM (Fig. 6A). After the polymerization by employing TLIRP for 15 h, the TEM image of PMMA-g-SiO₂ nanocomposites is showed in Fig. 6B. It is clearly revealed that the core-shell type morphology was produced successfully. The SiO₂ nanoparticles are visible as dark contrast areas and look dispersed uniformly throughout

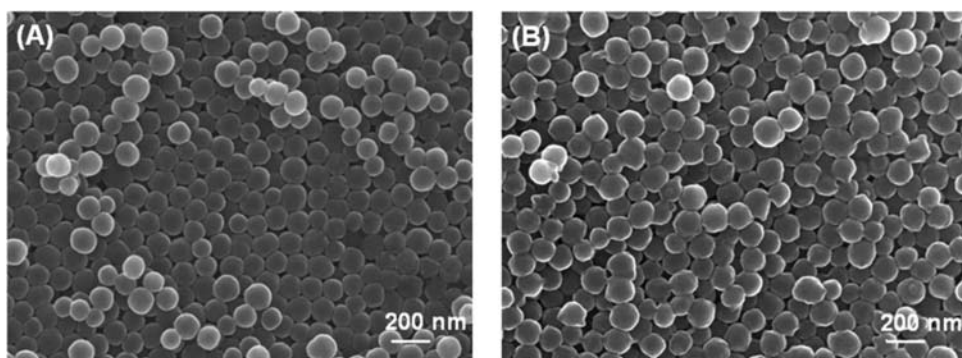


Figure 7. SEM images of (A) bare SiO₂ nanoparticles, and (B) PMMA-g-SiO₂.

Table 1. Results of DLS Measurements of Silica Particles.

No	Sample	Size(nm)
1	SiO ₂	103
2	SiO ₂ -SH	111
3	PMMA-g-SiO ₂ (5h)	158
4	PMMA-g-SiO ₂ (10h)	241
5	PMMA-g-SiO ₂ (15h)	312

the film, while the light PMMA shell formed fringes surrounding the SiO₂ cores. After polymerization, the size of nanoparticles has been increased significantly.

SEM images also provide additional information regarding the structure and morphology of the pure and modified silica nanoparticles as demonstrated in Fig. 7. These images demonstrate that both pure and modified nanoparticles have a uniform size and spherical shape. It is also clearly observed that there is no agglomeration of nanoparticles upon surface modification of SiO₂ nanoparticles by PMMA. The sizes of pure SiO₂ nanoparticles and PMMA-g-SiO₂ nanocomposites are found to be 108 nm and 142 nm, respectively.

Hydrodynamic diameters of the nanoparticles at different polymerization time were measured by DLS as shown in Table 1. The results indicate that the size of the nanoparticles become larger while polymerization time is increased. The diameter of the PMMA-g-SiO₂ nanocomposites were increased the average particle size from 158 to 312 nm when the polymerization time was increased from 5 to 15 h, which is consistent with the increase in the molecular weight of the PMMA as a function of time as observed during GPC analysis. For comparative analysis, DLS measurement of the pristine SiO₂ and corresponding SiO₂-SH was accomplished and observed that the average diameters of the pristine SiO₂ and SiO₂-SH were 103 and 111 nm, respectively.

Conclusions

The surface functionalization of SiO₂ nanoparticles with PMMA was accomplished *via* TLIRP of MMA in the presence of SiO₂-SH and BL. The grafting of PMMA on SiO₂ nanoparticles was confirmed by FT-IR and XPS analyses. The GPC analysis suggested that the molecular weight of the PMMA was increased with increasing the monomer conversion and it could be controlled with the polymerization time. The DLS measurement revealed that hydrodynamic diameter of the nanoparticles was also a function of the polymerization time. The TGA investigation showed the presence of PMMA in the nanocomposites by the *grafting from* approach. Moreover, it was observed that the thermal stability of the grafted PMMA improved by the incorporation of SiO₂ nanoparticles. The TEM image of PMMA-g-SiO₂ nanocomposites provided a clear snap shoot of the core-shell morphology of the hybrid compounds. The SEM images revealed that the PMMA modified nanoparticles have a uniform size and spherical shape without agglomeration.

Acknowledgments

This work was financially supported by the Joint Program of Cooperation in Science and Technology through NRF grant funded by the MEST (no. 2011-0025680) and the grant

from the Industrial Source Technology Development Program (Project No.10035163) of the Ministry of Knowledge Economy (MKE) of Korea.

References

- [1] Pyun, J., Jia, S., Kowalewski, T., Patterson, G. D., & Matyjaszewski, K. (2003). *Macromolecules.*, 36, 5094.
- [2] Sanchez, C., Soler-Illia, G. J. A., Ribot, F., Lalot, T., Mayer, C. R., & Cabuil, V. (2001). *Chem. Mater.*, 13, 3061.
- [3] Yuvaraj, H., Shim, J. J., & Lim, K. T. (2010). *Polym. Adv. Technol.*, 21, 424.
- [4] Chae, J., Kim, D. Y., Kim, S., & Kang, M., (2010). *J. Ind. Eng. Chem.*, 16, 906.
- [5] Ohno, K., Morinaga, T., Takeno, S., Tsujii, Y., & Fukuda, T. (2006). *Macromolecules.*, 39, 1245.
- [6] Park, E. J., Kim, W. S., Hwang, H. S., Park, C., & Lim, K. T. (2007). *Macromol. Symp.*, 249–250, 196.
- [7] Yoshinaga, K., Fujiwara, K., Mouri, E., Ishii, M., & Nakamura, H. (2005). *Langmuir*, 21, 4471.
- [8] Park, J. T., Seo, J. A., Ahn, S. H., Kim, J. H., & Kang, S. W., (2010). *J. Ind. Eng. Chem.*, 16, 517.
- [9] Ernest, A.D., & Lamb, D.W. (2005). *Journal of Phys: Conf. Series*, 15, 270–275.
- [10] Ohno, K., Morinaga, T., Koh, K., Tsujii, Y., & Fukuda, T. (2005). *Macromolecules.*, 38, 2137.
- [11] Chevigny, C., Gimes, D., Bertin, D., Schweins, R., Jestin, J., & Bou, F. (2011). *Polym. Chem.*, 2, 567.
- [12] Liu, C. H., & Pan, C. Y. (2007). *Polymer.*, 48, 3679.
- [13] Barbey, R., Lavanant, L., Paripovic, D., Schuwer, N., Sugnaux, C., Tugulu, S., & Klok, H. A. (2009). *Chem. Rev.*, 109, 5437.
- [14] Hwang, H. S., Bae, J. H., Kim, H. G., & Lim, K. T. (2010). *Eur. Polym. J.*, 46, 1654.
- [15] Rashid, M. H., Bae, J. H., Park, C., & Lim, K. T. (2010). *Mol. Cryst. Liq. Cryst.*, 532, 514.
- [16] Stober, W., Fink, A., & Bohn, E. J. (1968). *Colloid Interf. Sci.*, 26, 62.
- [17] Hu, M., Noda, S., Okubo, T., Yamaguchi, Y., & Komiyama, H. (2001). *Appl. Sur. Sci.*, 181, 307.